

STUDIES OF VIRUS STRUCTURE BY RAMAN SPECTROSCOPY

I. R17 VIRUS AND R17 RNA*

K.A. Hartman⁺, N. Clayton⁺ and G.J. Thomas, Jr.[#]

Received December 28, 1972

Summary. The laser-excited Raman spectrum of the RNA virus, R17, is shown to contain a large number of Raman lines assignable to scattering by vibrations of the nucleotide residues of RNA and the amino-acid residues of protein capsomers. The Raman lines from specific nucleotide vibrations in the phage are compared with their counterparts in the spectrum of protein-free RNA to suggest many similarities of RNA structure in the phage and protein-free states. However, the average configuration of guanine residues in the phage is apparently very different from that of protein-free RNA, suggesting that guanine plays an important role in RNA-protein interactions.

Introduction. Small RNA-containing viruses consist of one molecule of RNA enclosed by an external coat (capsid) made of protein subunits (capsomers). In the class of nearly spherical viruses, such as the phage R17, the capsomers are arranged on the surface of an icosahedron (1). The RNA molecule might simply reside in the cavity of the capsid, with few protein-RNA interactions. In this case the secondary structure of RNA in the virus could be quite similar to the secondary structure of RNA in solution. Alternatively, the RNA molecule may follow a proscribed path and reside between adjacent capsomers. In this case, the secondary and tertiary structures of RNA in the virus could be significantly different from the structure of RNA in solution.

*Supported by N.S.F. Grant BG 29289, by a Sigma Xi Grant-In-Aid of Research, by the University of Rhode Island and by Southeastern Massachusetts University.

⁺Department of Biophysics, University of Rhode Island, Kingston, R.I. 02881.

[#]Department of Chemistry, Southeastern Massachusetts University, North Dartmouth, Massachusetts 02747.

The most extensively studied RNA viruses are tobacco mosaic virus (TMV) and turnip yellow mosaic virus (TYMV). X-ray data suggest that the RNA of TMV follows a helical path between capsomers and that the RNA of TYMV follows a complex path which interlaces the capsomers (2). Further details of the conformations of RNA molecules in these and other viruses remain obscure and require investigation by different physico-chemical techniques.

Raman spectroscopy has provided a sharp tool for studying the conformations of nucleic acids and proteins in aqueous solutions and has been applied to rRNA (3), tRNA (4), lysozyme (5), ribonuclease (6) and insulin (7). We report here the Raman spectrum of the RNA phage R17 to show that the Raman spectrum contains information useful in answering questions about the structures of RNA and protein components of a virus.

Experimental Methods. The R17 phage were grown on *E. coli* K-12 Hfr Hayes and were isolated by a modified method of Gesteland and Boedtke (8). After precipitation with CH_3OH , the phage were re-suspended in 0.2N NaCl and given several cycles of centrifugation at 20,000g to remove sediment and at 100,000g to pellet the phage. The final pellet was suspended to 56.3 mg phage/ml in 0.2N NaCl solution for Raman spectroscopy. Plaque assays and sedimentation profiles were obtained on the phage before and after laser illumination in the Raman spectrometer and showed that no significant changes occurred as a result of exposure to the laser radiation.

RNA was extracted with phenol from R17 and was dissolved to 37 mg/ml in 0.2N NaCl solution for Raman spectroscopy. Further details of sample-handling and instrumentation are described elsewhere (3,4).

Results. Raman spectra of virus and RNA in 0.2N NaCl solutions (pH 7) are shown in Fig. 1. Of special importance is the absence

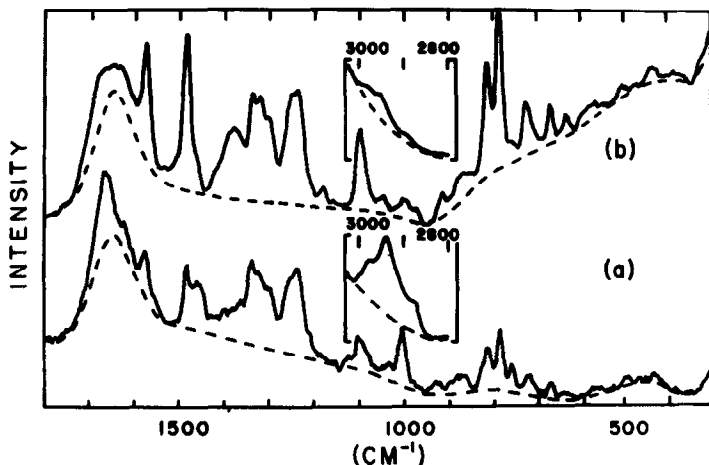


Figure 1. (a) Raman spectrum of R17 virus in aqueous 0.2N NaCl. Conditions: concentration $C=56.3$ mg phage/ml ($=17.8$ mg RNA/ml), pH=7, $t=32^{\circ}\text{C}$, spectral slit width $\Delta\sigma=10\text{ cm}^{-1}$, period $\tau=20$ sec, rate of scan $r=25\text{ cm}^{-1}/\text{min}$, amplification $a=1\times$ (inset $a=1/3\times$) (b) Raman spectrum of R17 RNA in aqueous 0.2N NaCl. Conditions: $C=37$ mg RNA/ml, pH=7, $t=32^{\circ}\text{C}$, $\Delta\sigma=10\text{ cm}^{-1}$, $\tau=20$ sec, $r=25\text{ cm}^{-1}/\text{min}$, $a=1\times$ (inset $a=1/3\times$). The solid curves shown are the spectra as recorded and the dashed curves indicate the background of scattering by liquid H_2O . The volume concentration of RNA in (b) is 2.2 times greater than that in (a).

of a steeply sloping background in the recorded spectra. However, the spectrum of phage contains a slightly sloping baseline (upward with increasing Raman frequency) which alters the appearance of the normal background of liquid H_2O in the region below 800 cm^{-1} . The Raman frequencies, relative intensities and assignments (5,9) for each spectrum are given in Table I.

Table I

Raman Frequencies, Relative Intensities and Assignments^a

R17-RNA		R17-Virus	
Frequency	Assignment	Frequency	Assignments
			RNA Protein
		~350(0)	r,C
		385(0)	C
435(1)	r	435(1)	r ?
502(0)	G,C	500(1)	G,C disulfide
580(1B)	C,G	575(1)	C,G Trp
635(1)	r	637(1)	r disulfide
670(2)	G	670(2)	G
710(S)	A	710(S)	A
725(3)	A	722(3)	A
755(0)	C	760(3)	Trp
787(10)	C,U	787(8)	C,U
815(7)	P	815(6)	P
		830(S)	Tyr
860(0)	r	865(3)	Trp
880(0)	r	885(S)	Trp
915(1)	r		
975(0)	r	930(1)	Trp
1001(1)	A,U,C	1005(7)	Phe
		1015(S)	Trp
1045(1)	r	1035(1)	Phe
		1085(S)	Phe
1100(5)	P	1100(5)	P
		1125(1)	?
1160(0)	r	1162(0)	r
1180(1)	C,G,A	1180(0)	C,G,A
		1210(S)	Tyr, Phe
1238(6)	U,C	1238(10)	U,C Am III
1250(6)	C,U	1250(8)	C,U Am III
		1268(S)	Am III
1303(4)	A,C	1300(S)	A,C
1320(6)	G	1320(S)	G
1342(6)	A	1343(6)	A Trp
		1365(2B)	G Trp
1380(4B)	G,U,A	1400(1)	U,A
		1450(S)	C-H def
1462(0)	C-H def	1462(4)	
1482(10)	G,A	1480(5)	G,A
1535(0)	G	1550(S)	Trp
1575(7)	G,A	1575(5)	G,A Trp
		1600(1)	?
1620(B)	U	1620(2)	U Trp,Tyr,Phe
~1650(B)	U,G,C	1665(B)	U,G,C Am I
~1685(B)			
2890(1)	aliphatic	2880(10B)	aliphatic
2955(6)		2942(30B)	
2980(3)		2975(15B)	
	C-H str		C-H str

^aFrequencies in cm^{-1} are accurate to $\pm 3 \text{ cm}^{-1}$ for sharp lines and $\pm 5 \text{ cm}^{-1}$ for weak or broad lines. Relative intensities, in parentheses, are based upon an arbitrary intensity of 10 given to the strongest line in each spectrum below 1600 cm^{-1} . Details of assignments are given in references 5 and 9. Abbreviations: A adenine, U uracil, G guanine, C cytosine, r ribose, P phosphate, Trp tryptophan, Tyr tyrosine, Phe phenylalanine, Am amide, str stretching, def deformation, S shoulder and B broad.

Discussion. Raman lines characteristic of both RNA and protein components are resolved in the spectrum of the virus (Fig. 1a). The most intense lines occur in the region $2800-3000\text{ cm}^{-1}$, due mainly to aliphatic C-H stretching vibrations of amino acid-side chain residues. Raman scattering by proteins also dominates the $1600-1700\text{ cm}^{-1}$ interval where amide I vibrations of the peptide groups exhibit greater Raman intensity than the carbonyl group vibrations of U, G and C nucleotides. This is expected since the protein is 68.3% by weight of the R17-viron (2). In the region $250-1600\text{ cm}^{-1}$ RNA and protein residues give rise to Raman lines of comparable intensities.

Raman lines at 670, 722, 787, 815, 1100 and 1480 cm^{-1} , all due to vibrations of RNA subgroups, are best suited to quantitative intensity measurement in the spectrum of the virus. For comparison of these intensities with those of protein-free RNA (Table II), the former are multiplied by a factor of 2.2 which corrects for the different volume concentrations of RNA in the two samples. (See Fig. 1 legend). Table II shows that the intensity of the 1100 cm^{-1} line, so corrected, is the same for phage RNA and protein-free RNA. This is expected since the 1100 cm^{-1} line (which results from the symmetric PO_2^- stretching vibration) is largely insensitive to changes in RNA conformation (9-11).

Table II also indicates that the RNA lines at 670 and 722 cm^{-1} have the same intensity values for phage and protein-free states. The lines at 787 and 815 cm^{-1} appear somewhat weaker in the phage than in the protein-free RNA, but the intensity differences are close to the experimental uncertainties. The line at 1480 cm^{-1} , however, is clearly far weaker in phage RNA than in protein-free RNA and presumably reflects a change in RNA secondary structure imposed by the viral proteins.

Table II

Selected Raman Intensities (Arbitrary Units) of R17-RNA in
Phage and Protein-Free States

cm^{-1} (assignment)	Intensity in Phage RNA ^a	Intensity in Protein-Free RNA ^b
670(G)	37	35
722(A)	44	47
787(C,U) ^c	150	162
815(P)	97	112
1100(P)	86	83
1480(G,A) ^d	84	159

^aAverage values from 3 scans at the conditions of Fig. 1a, after multiplication by 2.2 (See text). Experimental uncertainties are $\pm 10\%$

^bFrom Fig. 1b; experimental uncertainties $\pm 3\%$.

^cThe contributions of C and U are approximately 60% and 40%, respectively, to the total intensity.

^dThe contributions of G and A are approximately 70% and 30%, respectively, to the total intensity.

The peptide groups of the phage proteins give intense Raman lines in the amide I (1665 cm^{-1}) and amide III (1238 , 1250 and 1268 cm^{-1}) regions, which are close to the amide frequencies reported for other proteins (5, 7). Additional Raman lines from amino acid-side chain residues and U and C nucleotides also complicate the spectrum in this region (7). The tryptophan residues are conspicuous by their characteristic ring frequencies at 760 and 1015 (shoulder) cm^{-1} and the phenylalanine residues by their ring mode at 1005 cm^{-1} . The 1005 and 1015 cm^{-1} components were

easily resolved by Lord and Yu (5) in spectra of lysozyme at higher resolution.

The Raman intensities at 500 and 636 cm^{-1} in Fig. 1a, which are far greater than expected from RNA alone, are attributed predominantly to S-S and C-S bond stretching vibrations of disulfide linkages between the chains of phage protein (5).

Conclusions. The Raman intensities at 815 and 1100 cm^{-1} are sensitive indices of the RNA-backbone conformation and those at 722, 787 and 1480 cm^{-1} are proportional to the extent of participation of A, U+C and G residues, respectively, in RNA-secondary structure (3,4,9-12). The data of Table II therefore indicate similarities in structure and molecular environment of the RNA backbone and its nucleotides, excepting G, in the phage and protein-free states. However, a gross change in the molecular configuration of G residues is apparent between the phage and protein-free states. Guanine obviously plays an important role in RNA-protein interactions in the virus. Further studies to determine the nature of this interaction and the results of more refined intensity measurements will be reported in a subsequent paper.

The present results indicate that the Raman spectrum of a native virus can reveal many characteristic vibrations of both its protein and nucleic acid components and that Raman spectroscopy is therefore a feasible method for the study of virus structure in an aqueous environment. The technique may also be applied to other nucleoproteins, such as ribosomes and chromosomes.

References.

1. C.R. Goodheart, An Introduction to Virology. W.B. Saunders, Co., Philadelphia, 1969.
2. J.M. Kaper, in Molecular Basis of Virology (H. Fraenkel-Conrat, ed.). Reinhold, N.Y., 1968.

3. G.J. Thomas, Jr., G.C. Medeiros and K.A. Hartman, *Biochem. Biophys. Res. Commun.* 44, 587 (1971).
4. G.J. Thomas, Jr., G.C. Medeiros and K.A. Hartman, *Biochim. Biophys. Acta* 277, 71 (1972).
5. R.C. Lord and N.T. Yu, *J. Mol. Biol.* 50, 509 (1970).
6. R.C. Lord and N.T. Yu, *J. Mol. Biol.* 51, 203 (1970).
7. N.T. Yu, C.S. Liu and D.C. O'Shea, *J. Mol. Biol.* (in press).
8. R.F. Gesteland and H. Boedtker, *J. Mol. Biol.* 8, 496 (1964).
9. G.J. Thomas, Jr., *Biochim. Biophys. Acta* 213, 417 (1969).
10. L. Lafleur, J. Rice and G.J. Thomas, Jr., *Biopolymers* (in press).
11. G.J. Thomas, Jr. and K.A. Hartman (manuscript in preparation).
12. E.W. Small and W. Peticolas, *Biopolymers* 10, 1377 (1971).